# Visual-Salience-Based Tone Mapping for High Dynamic Range Images

Zhengguo Li, Senior Member, IEEE, and Jinghong Zheng

Abstract—Visual saliency aims to predict the attentional gaze of observers viewing a scene, and it is thus highly demanded for tone mapping of high dynamic range (HDR) images. In this paper, novel saliency-aware weighting and edge-aware weighting are introduced for HDR images. They are incorporated into an existing guided image filter to form a perceptually guided image filter. The saliency-aware weighting and the proposed filter are applied to design a new local tone-mapping algorithm for HDR images such that both extreme light and shadow regions can be reproduced on conventional low dynamic range displays. In particular, the proposed filter is applied to decompose the luminance of the input HDR image into a base layer and a detail layer. The saliency-aware weighting is then adopted to design a saliency-aware global tone mapping for the compression of the base layer. The proposed filter preserves sharp edges in the base layer better than the existing guided filter. Halo artifacts are thus significantly reduced in the tone-mapped image. Moreover, the visual quality of the tone-mapped image, especially attention-salient regions, is improved by the saliency-aware weighting.

*Index Terms*—Edge-aware weighting, high dynamic range (HDR), local filtering, saliency-aware weighting, tone mapping.

## I. INTRODUCTION

CONVENTIONAL low dynamic range (LDR) image A represents a scene at an exposure level with a limited contrast range. This results in loss of details in bright or dark areas of the scene depending on the setting of exposure level. A high dynamic range (HDR) image overcomes the limitation of the LDR image, and it can preserve details in both the bright and dark areas of the scene well [1]. Therefore, an HDR image includes much more information than an LDR image. However, the display of an HDR image is an issue. Most current conventional display devices only have limited dynamic ranges and hence are unable to display HDR images. Due to the huge discrepancy between the ranges of HDR images and display devices, it is necessary to compress HDR images such that the appearance of both extremes of light and shadow regions can be reproduced on these ordinary LDR display devices simultaneously. On the other hand, investigations show that our human visual system (HVS) is overwhelmed by a tremendous amount of visual information which it cannot process completely [2]. Visual saliency reflects how much an image region or object

Manuscript received November 10, 2013; revised January 6, 2014 and February 11, 2014; accepted February 24, 2014. Date of publication March 27, 2014; date of current version September 12, 2014.

The authors are with the Institute for Infocomm Research, 138632 Singapore (e-mail: ezgli@i2r.a-star.edu.sg; jzheng@i2r.a-star.edu.sg).

Color versions of one or more of the figures in this paper are available online at http://ieeexplore.ieee.org.

Digital Object Identifier 10.1109/TIE.2014.2314066

stands out from its surrounding and provides a mechanism for prioritizing visual processing [3]. Visual saliency was widely applied for the processing of the conventional LDR images, such as image/video compression, visual search, object recognition, etc. [4]–[10]. Since visual saliency aims to predict the attentional gaze of observers viewing a scene, it is highly demanded for the HDR images, especially for the display of the HDR images.

To display the HDR images on the LDR display devices, many global and local tone-mapping algorithms were developed [11]. A global tone-mapping algorithm is simple and preserves naturalness of an HDR image because a global tonemapping algorithm compresses an HDR image using a monotonic curve [11]. However, the global tone-mapping algorithms face a fundamental difficulty in preserving the fine details of an HDR image [12]. Many local tone-mapping algorithms were proposed to address the problem, and they focused on avoiding halo artifacts from appearing in the tone-mapped images. Reinhard et al. [13] proposed a spatially varying operator that is akin to "dodging and burning" in photography [14]. The locality of neighborhood is obtained by using a circular filter whose size is adapted for each pixel by computing a measure of local fine details. Farbman et al. [15] employed a quadratic-optimization-based edge-preserving image smoothing technique to decompose the luminance of an HDR image into a base layer and a detail layer. The base layer consists of large-scale variations such as sharp edges, while the detail layer is composed of small-scale variations such as fine details. The base layer is scaled down using a scale factor in logarithm domain to reduce the dynamic range. Even though the globaloptimization-based approaches often yield excellent quality, they have high computational cost. Durand and Dorsey [16] presented a fast local mapping by using a bilateral filter [17] to decompose the luminance of an HDR image into a base layer and a detail layer. He et al. [18] introduced a guided filter for the decomposition of an HDR image. However, the local filteringbased methods cannot preserve sharp edges like the globaloptimization-based approaches [15], [18]. As such, halos are unavoidable for local filters when they are adopted to smooth some edges [18]. It is thus desired to design a new local filter that can preserve sharp edges better so as to avoid halo artifacts from appearing in final images. In addition, visual saliency provides a mechanism for prioritizing visual processing, and it is shown to be useful for the processing of the conventional LDR images [6], [19]-[21], [23]. It could be expected that visual saliency, like other perceptual quality measures such as perceived local contrast and color saturation in [24], is useful

for HDR images. Unfortunately, it is not well utilized in the existing local tone-mapping algorithms. It is therefore also desired to build up a local tone-mapping algorithm by taking visual saliency into consideration.

In this paper, a saliency-aware local tone-mapping algorithm is introduced for HDR images. Among the existing saliency models in [19]-[23], the saliency model in [22] and [23] is chosen to be extended from LDR domain to HDR domain due to its simplicity and robustness. The extended saliency model is adopted to set up a saliency-aware weighting for the processing of HDR images. The proposed saliency-aware weighting and a new edge-aware weighting are fused together to build up a content-aware weighting which is incorporated into the guided image filter in [18] to form a perceptually guided image filter. The new filter and the saliency-aware weighting are then applied to design a local mapping algorithm for HDR images. The three major components of the proposed local tone-mapping algorithm are the decomposition of the HDR luminance component into a base layer and a detail layer, the compression of the base layer, and the amplification of the detail layer. The proposed filter is applied for the decomposition of the luminance component of an HDR image. Since the proposed filter preserves sharp edges in the base layer better than the guided filter in [18], halo artifacts are significantly reduced in the tone-mapped image. The proposed saliencyaware weighting is adopted to design a saliency-aware global tone-mapping algorithm for the compression of the base layer. In particular, it is incorporated into the tone-mapping algorithm in [25] to form such a tone-mapping algorithm. The algorithm in [25] is selected due to its outstanding performance. The tone-mapped results in [25] can reproduce the overall appearance of the real-world scenes which make Reinhard's method close to global mapping algorithms in terms of image naturalness. It was shown in [26] that Reinhard's photographic tone reproduction [25] is one of the best local tone-mapping algorithms. Overall, the three major contributions of this paper are the following: 1) a simple saliency-aware weighting for HDR images; 2) a content-aware guided image filter; and 3) a seamless integration of the extend saliency-aware weighting and the global tone-mapping algorithms in [25]. Experimental results show that the proposed local tone-mapping algorithm can improve the visual quality of the tone-mapped image, especially attention-salient regions.

This paper is organized as follows. Section II contains both the saliency-aware weighting and the edge-aware weighting. The proposed weighting is applied in Section III to design a local mapping algorithm for HDR images. Experimental results are presented in Section IV to verify the efficiency of the proposed tone-mapping algorithm. Finally, concluding remarks are provided in Section V.

# II. CONTENT-AWARE WEIGHTING

In this section, the saliency model in [22] and [23] is first extended to build up a saliency-aware weighting for an HDR image  $[\Gamma_b(p')]$ . An edge-aware weighting  $\Gamma_e(p')$  is then proposed for an HDR image by using the local variance and the

local mean value of the HDR image. The proposed contentaware weighting is then computed as

$$W(p') = \frac{\Gamma_e(p')}{\Gamma_h(p')}. (1)$$

# A. Saliency-Aware Weighting

Let  $I_h(p') = [R_h(p'), G_h(p'), B_h(p')]$  be a pixel in an HDR image. Similar to the saliency model in [22] and [23], our saliency model for the HDR image is based on the image cooccurrence histogram (ICH) of the HDR image. Since each color component of the HDR image is usually represented by floating numbers, it is first quantized such that it is represented by integers. For simplicity, the total number of bins is denoted as K, and the color component  $R_h$  is taken as an example to illustrate the process. The quantized color component is denoted as  $Q(R_h(p'))$ . The ICH of the color component  $R_h$  in intensity domain  $H_{i,R}(m,n)$ , which represents the occurrence/cooccurrence of pixel intensity, is defined as

$$H_{i,R} = [H_{i,R}(m,n)]; 1 \le m, n \le K$$

where  $H_{i,R}$  is a symmetric square matrix of size  $K \times K$ . Let  $\Omega_{\rho_1}(p')$  be a square window centered at the pixel p' of a radius  $\rho_1$ . The value of  $\rho_1$  is selected as 4 in this paper. An ICH element  $H_{i,R}(m,n)$  is the cooccurrence count of image values m and n within the window  $\Omega_{\rho_1}(p')$ . A probability mass function (PMF)  $P_{i,R}$  is then obtained by normalizing the ICH matrix  $H_{i,R}$ . Since saliency is usually negatively correlated with occurrence/cooccurrence, an inverted PMF  $\bar{p}_{i,R}(m,n)$  is computed as

$$\begin{cases} 0; & \text{if } P_{i,R}(m,n) = 0 \\ 0; & \text{if } P_{i,R}(m,n) > \frac{1}{U_{i,R}} \\ \frac{1}{U_{i,R}} - P_{i,R}(m,n); & \text{if } P_{i,R}(m,n) \leq \frac{1}{U_{i,R}} \end{cases}$$

where  $P_{i,R}(m,n)$  is an element of  $P_{i,R}$  and  $U_{i,R}$  is the total number of nonzero items in  $H_{i,R}$ . Visual saliency is computed from the inverted PMF. For a pixel p', visual saliency  $S_{i,R}(p')$  is defined as follows:

$$S_{i,R}(p') = \sum_{p \in \Omega_{p_1}(p')} \bar{p}_{i,R}\left(Q\left(R_h(p')\right), Q\left(R_h(p)\right)\right).$$

Similarly,  $S_{i,G}(p')$  and  $S_{i,B}(p')$  are computed for the color component  $G_h$  and the color component  $B_h$ . All of them are normalized to [0, 1] and added together to form the saliency model  $S_i(p')$  in intensity domain. Besides the saliency computed in intensity domain, gradient orientation is also incorporated in the saliency computation. For each pixel, the gradient orientation is calculated and quantized to 180 bins. An orientation cooccurrence histogram  $H_{o,R}$  can be constructed from the quantized gradient orientation. The corresponding inverted PMF  $\bar{P}_{o,R}$  and the saliency model  $S_{o,R}(p')$  can then be generated from  $H_{o,R}$ . Similarly,  $S_{o,G}(p')$  and  $S_{o,B}(p')$  are computed. All of them are normalized to [0, 1] and added together to form the saliency model  $S_o(p')$  in gradient domain.

The sum of  $S_i(p')$  and  $S_o(p')$  is denoted as S(p'). The final visual saliency is defined as the normalized value of S(p')

$$S_F(p') = \frac{1}{N} \sum_{p=1}^{N} \frac{S(p')}{S(p)}$$

where N is the total number of pixels in an image.

The proposed saliency-aware weighting  $\Gamma_b(p')$  is then defined as

$$\Gamma_b(p') = \begin{cases} 1; & \text{if } S_F(p') \le 1\\ S_F^{\kappa}(p'); & \text{otherwise} \end{cases}$$
 (2)

where  $\kappa$  (typically between 0.5 and 1) is a constant and its value is selected as 0.75 in this paper.

The processing priority of the pixel p' is assigned according to the value of  $\Gamma_b(p')$ . A higher priority is assigned to a pixel with a larger  $\Gamma_b(p')$ . The value of  $\Gamma_b(p')$  is usually larger than 1 if the pixel p' is in an attention-salient region. Therefore, a higher priority is usually given to a pixel in an attention-salient region. This matches the feature of our HVS, i.e., our HVS pays more attention to the information in attention-salient regions than that outside the attention-salient regions [19].

# B. Edge-Aware Weighting

The luminance value of the HDR image is first obtained by computing a linear combination of the red, green, and blue components as follows:

$$Y_h(p) = 0.299R_h(p) + 0.587G_h(p) + 0.114B_h(p).$$
 (3)

The luminance component in log domain is denoted as  $L_h(p)$ . Let  $\sigma_{L_h,\rho_2}^2(p)$  and  $\mu_{L_h,\rho_2}(p)$  be the variance and the mean value of the component  $L_h$  in the window  $\Omega_{\rho_2}(p)$ . The value of  $\rho_2$  is selected as 15 in this paper. Consider two pixels p and p'. If  $L_h(p)$  is at an edge and  $L_h(p')$  is in a flat area, the value of  $\sigma_{L_h,\rho_2}^2(p)/\mu_{L_h,\rho_2}^2(p)$  is usually larger than that of  $\sigma_{L_h,\rho_2}^2(p')/\mu_{L_h,\rho_2}^2(p')$ . Based on this observation, an edge-aware weighting  $\Gamma_e(p')$  is computed by using normalized local variances of all pixels, i.e.,

$$\Gamma_e(p') = \frac{1}{N} \sum_{p=1}^{N} \frac{\left(\frac{\sigma_{L_h,\rho_2}^2(p') + \nu_1}{\mu_{L_h,\rho_2}^2(p') + \nu_2}\right)^{\zeta}}{\left(\frac{\sigma_{L_h,\rho_2}^2(p) + \nu_1}{\mu_{L_h,\rho_2}^2(p) + \nu_2}\right)^{\zeta}}$$
(4)

where  $\zeta$  (typically between 0.5 and 1) is a constant and its value is selected as 0.75. The constant  $\nu_1$  is included to avoid instability when  $\sigma_{L_h,\rho_2}^2(p)$  is close to zero, and its value is computed as  $(0.001*L)^2$ , with L being the dynamic range of the input image [27].  $\nu_2$  is a small constant (typically  $10^{-9}$ ) that prevents division by zero.

The value of  $\Gamma_e(p')$  is usually larger than 1 if p' is at an edge and smaller than 1 if p' in a smooth area. Clearly, larger weighting is assigned to a pixel at an edge than a pixel in a flat area by using the proposed weighting  $\Gamma_e(p')$  in (4).

#### III. SALIENCY-AWARE LOCAL TONE MAPPING

Psychophysical studies indicate the following: 1) Our HVS appears to select attention-salient regions before further processing so as to reduce the complexity of the scene analysis, and 2) our HVS is not blind to the information outside the attention-salient regions [19]. Therefore, it makes sense to allow distortions according to the visual saliency model to take place after the dynamic range of the HDR image is scaled down.

Given an HDR image, the luminance component of the HDR image in (3) is decomposed as

$$Y_h(p) = Y_b(p)Y_d(p) \tag{5}$$

where  $Y_b$  and  $Y_d$  are the base layer and the detail layer, respectively. The dynamic range of the detail layer  $Y_d$  is small, while the base layer  $Y_b$  could vary a great deal, often much more than the detail layer  $Y_d$ . The overall dynamic range is reduced by using a global tone-mapping algorithm to scale down the base layer  $Y_b$  as  $\hat{Y}_b$ . The detail layer  $Y_d$  is preserved or even amplified as  $\hat{Y}_d$  to enhance local contrasts. The compressed luminance value  $Y_l$  is the product of  $\hat{Y}_b$  and  $\hat{Y}_d$ . The HDR image  $\{R,G,B\}_h$ ,  $Y_h$ , and  $Y_l$  are finally adopted to generate the output LDR image  $\{R,G,B\}_l$ .

As shown by the "just noticeable difference" experiment [28], the log function approximates the transformation performed by the retina of the HVS. Inspired by this fact, the decomposition is performed in the log domain as

$$L_h(p) = L_b(p) + L_d(p) \tag{6}$$

where  $L_b(p)$  and  $L_d(p)$  are  $\log(Y_b(p))$  and  $\log(Y_d(p))$ , respectively.

The three major components of the proposed local tone-mapping algorithm are the following: 1) the decomposition of  $L_h$  into  $L_b$  and  $L_d$ ; 2) the compression of  $L_b$  via a global tone mapping; and 3) the amplification of  $L_d$ .

# A. Decomposition of $L_h$ by a Perceptually Guided Filter

Inspired by the guided filter in [18],  $L_b$  is assumed to be a linear transform of  $L_h$  in the window  $\Omega_{\rho_2}(p')$ 

$$L_b(p) = a_{p'}L_h(p) + b_{p'}, \ \forall \ p \in \Omega_{\rho_2}(p')$$
 (7)

where  $a_{p'}$  and  $b_{p'}$  are supposed to be constant in the window  $\Omega_{\rho_2}(p')$ .

The linear coefficients  $(a_{p'}, b_{p'})$  are obtained by minimizing the difference between  $L_h$  and  $L_b$  while maintaining the linear model (7), i.e., by minimizing the following cost function:

$$\sum_{p \in \Omega_{p_2}(p')} \left[ W(p') \left( a_{p'} L_h(p) + b_{p'} - L_h(p) \right)^2 + \lambda a_{p'}^2 \right]. \quad (8)$$

By comparing the cost function  $E(a_{p'},b_{p'})$  in (8) with the cost function in [18], it can be found that the cost function  $E(a_{p'},b_{p'})$  in (8) contains a content-aware weighting W(p') which is responsible for reducing the halo artifact and preserving fine details according to the saliency-aware weighting. The value of  $\Gamma_e(p')$  is usually larger than 1 if p' is at an edge and

smaller than 1 if p' is in a flat area. This implies the following: 1) the fidelity of  $L_b$  with respect to  $L_h$  is required to be higher by the proposed filter if p' is at an edge, and 2) the base layer  $L_b$  is required to be smoother by the proposed filter if p' is in a flat area. Therefore, the proposed filter has a potential to preserve sharp edges and smooth flat regions better than the guided filter in [18]. In addition, the proposed filter can smooth attention-salient regions better than the guided filter in [18]. As a result, more fine details in the attention-salient regions are preserved in the tone-mapped image via the proposed filter.

It is shown in the linear model (7) that  $\nabla L_b(p) = a_{p'} \nabla L_h(p)$ . Clearly, the smoothness of  $L_b$  in  $\Omega_{\rho_2}(p')$  depends on the value of  $a_{p'}$ . This implies that the data terms and the regularization terms in (8) are similar to that in [15] in the sense that the data term measures the fidelity of  $L_b$  with respect to the input  $L_h$  and the regularization term is on the smoothness of  $L_b$ . The major difference is that the proposed filter and the filter in [18] are based on local optimization while the optimization problem in [15] is global.

The optimal values of  $a_{p'}$  and  $b_{p'}$  are computed as

$$a_{p'} = \frac{W(p')\sigma_{L_h,\rho_2}^2(p')}{W(p')\sigma_{L_h,\rho_2}^2(p') + \lambda}$$
(9)

$$b_{p'} = (1 - a_{p'})\mu_{L_h, \rho_2}(p'). \tag{10}$$

It is worth noting that a pixel p is involved in all overlapping windows  $\Omega_{\rho_2}(p')$ 's. There are many different values of  $L_b(p)$ . A simple method is to average all of the possible values of  $L_b(p)$  as follows:

$$L_b(p) = \bar{a}_p L_h(p) + \bar{b}_p \tag{11}$$

where  $\bar{a}_p$  and  $\bar{b}_p$  are computed as

$$\bar{a}_p = \frac{1}{|\Omega_{\rho_2}(p)|} \sum_{p' \in \Omega_{\rho_2}(p)} a_{p'} \tag{12}$$

$$\bar{b}_p = \frac{1}{|\Omega_{\rho_2}(p)|} \sum_{p' \in \Omega_{\rho_2}(p)} b_{p'}.$$
 (13)

# B. Compression of Base Layer $L_b$ via a Saliency-Aware Global Tone Mapping

The proposed saliency-aware weighting in (2) is adopted to design a saliency-aware global tone-mapping algorithm for the compression of the base layer  $L_b$ . The compression of the base layer  $L_b$  is important for the visual quality of the generated LDR image. Since edges are preserved in the base layer  $L_b$ , it is necessary to only reduce the magnitudes of edges while keeping their directions unaltered when the base layer  $L_b$  is compressed. Otherwise, the tone-mapped image will suffer from halo artifacts. The objective is achieved if the base layer  $L_b$  is compressed by using a global mapping algorithm. In this section, a simple saliency-aware global tone-mapping algorithm is proposed by incorporating the saliency-aware weighting in (2) into the global tone-mapping algorithm in [25].

The average value of  $L_h$  which is denoted as  $\bar{L}_h$  plays an important role in the tone-mapping algorithm in [13] and [25]. It is worth noting that all pixels are assigned the same weight when the value of  $\bar{L}_h$  is computed in [13] and [25]. The proposed saliency-aware weighting in (2) is now adopted to compute the value of  $\bar{L}_h$  as

$$\bar{L}_h = \frac{\sum_{p=1}^{N} \Gamma_b(p) L_h(p)}{\sum_{p=1}^{N} \Gamma_b(p)}.$$
 (14)

Let a be the overall key value of the whole HDR image, and it determines the overall brightness of the HDR image [13]. Same as [25], the value of a is given by

$$a = 0.18 * 4^{\frac{2\bar{L}_h - L_h^{\min} - L_h^{\max}}{L_h^{\max} - L_h^{\min}}}$$
 (15)

where  $L_h^{\rm max}$  and  $L_h^{\rm min}$  are the maximal and minimal values of all  $L_h(p) (\neq 0)$  in an HDR image, respectively. To improve stability, we exclude some of the brightest and dimmest pixels.

The base layer  $L_b$  is then compressed by

$$\hat{L}_b(p) = \log(a) + L_b(p) - \bar{L}_h - \log\left(1 + a\exp\left(L_b(p) - \bar{L}_h\right)\right).$$

Clearly, the overall brightness of the tone-mapped image heavily depends on attention-salient regions. The dynamic ranges of the attention-salient regions will be preserved better in the final image. As such, the visual quality of the regions is also improved compared with a tone-mapping algorithm without consideration of saliency-aware weighting.

# C. Amplification of Detail Layer $L_d$

It is also important to amplify the detail layer such that the final LDR image looks sharper. A simple method is proposed to achieve this as follows:

$$\hat{L}_d(p) = \theta L_d(p) \tag{16}$$

where  $\theta$  (typically between 1 and 2) is a constant and its value is chosen as 1.5 in this paper.

To display the tone-mapped image, the compressed  $\hat{L}_b$  and the processed  $\hat{L}_d$  are converted back into intensity domain as  $\hat{Y}_b(p)$  and  $\hat{Y}_d(p)$ , respectively. The tone-mapped luminance component  $Y_l$  is the product of the compressed base layer  $\hat{Y}_b$  and the amplified detail layer  $\hat{Y}_d$ . The color channels of an HDR image are then scaled by

$$\{R, G, B\}_l(p) = \left(\frac{Y_l(p)}{Y_h(p)}(R, G, B)_h(p)\right)^s$$
 (17)

where  $\{R,G,B\}_l$  denote the color channels of the output LDR image. The exponent s (typically between 0.375 and 0.625) is the saturation parameter with the value of 0.5 to correct the attenuation effect of display devices.

# IV. EXPERIMENTAL RESULTS

Tone mapping of HDR images is a very hot research topic in the fields of image processing and computation photography;

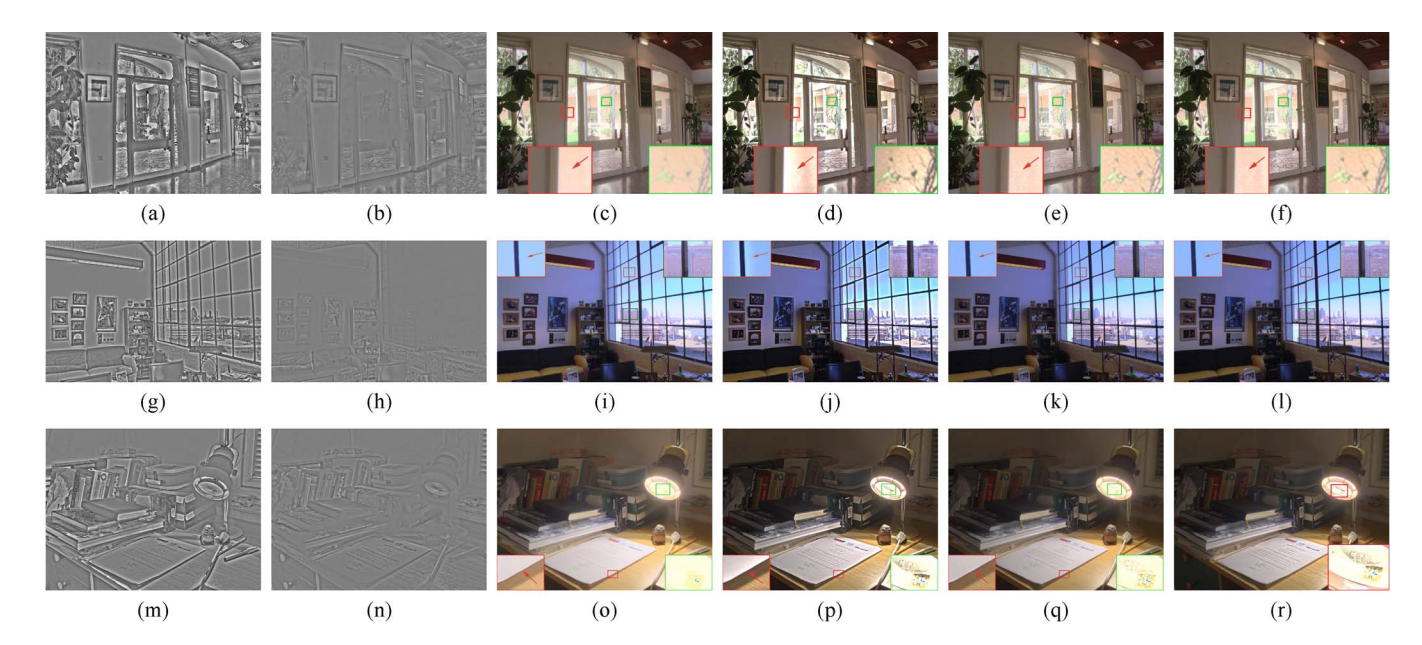


Fig. 1. Comparison on tone-mapped images. (a), (g), and (m) Extracted fine details by the filter in [18]. (b), (h), and (n) Extracted fine details by the proposed filter. (c), (i), and (o) Tone-mapped images by the algorithm in [13] and [25]. (d), (j), and (p) Tone-mapped images by the filter in [18]. (e), (k), and (q) Tone-mapped images by using the  $L_2$ -norm-based optimization method in [15]. (f), (l), and (r) Tone-mapped images by the proposed filter.

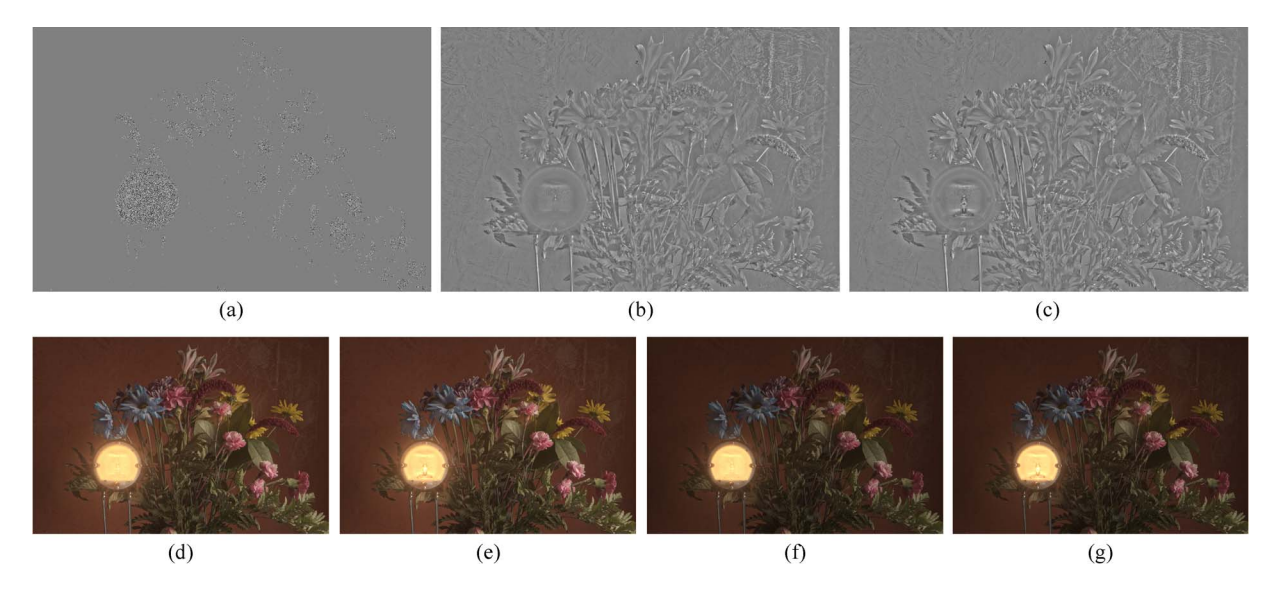


Fig. 2. Comparison of four different methods. (a) Saliency-aware weighting. (b) Extracted fine details without the proposed saliency-aware weighting. (c) Extracted fine details with the proposed saliency-aware weighting. (d) Tone-mapped image without saliency-aware weighting. (e) Tone-mapped image with incorporation of saliency-aware weighting in decomposition of  $L_h$ . (f) Tone-mapped image with incorporation of saliency-aware weighting in compression of base layer. (g) Tone-mapped image with incorporation of saliency-aware weighting in both decomposition of  $L_h$  and compression of base layer.

there are dozens of tone-mapping algorithms. Since this paper focuses on incorporating a saliency-aware weighting and an edge-aware weighting into tone mapping of HDR images, the proposed local mapping algorithm is only compared with two local mapping algorithms based on the quadratic optimization method in [15], the guided filter in [18], and the local tone-mapping algorithm in [13] and [25]. All results are compared from the visual quality point of view rather than from the objective quality metric in [29] point of view. Readers are invited to view to the electronic version of the full-size figures in order to better appreciate the differences among images in this paper.

The efficiency of the proposed edge-aware weighting in (4) is first tested by setting the value of  $\Gamma_b(p)$  as 1 and testing three sets of HDR images. The values of  $\rho$  and  $\lambda$  are, respectively, chosen as 15 and 1 for the filter in [18] and the proposed filter. As suggested in [15], the values of  $\gamma$ ,  $\epsilon$ , and  $\lambda$  are, respectively, chosen as 1.2, 0.001, and 2 for the global optimization method in [15]. The default settings of the algorithm in [13] and [25] are utilized to generate tone-mapped images. It is illustrated in Fig. 1 that the proposed filter preserves edges in the base layer much better than the guided filter in [18]. As a result, the proposed tone-mapping algorithm can avoid halo artifacts from appearing in the tone-mapped images, while there are

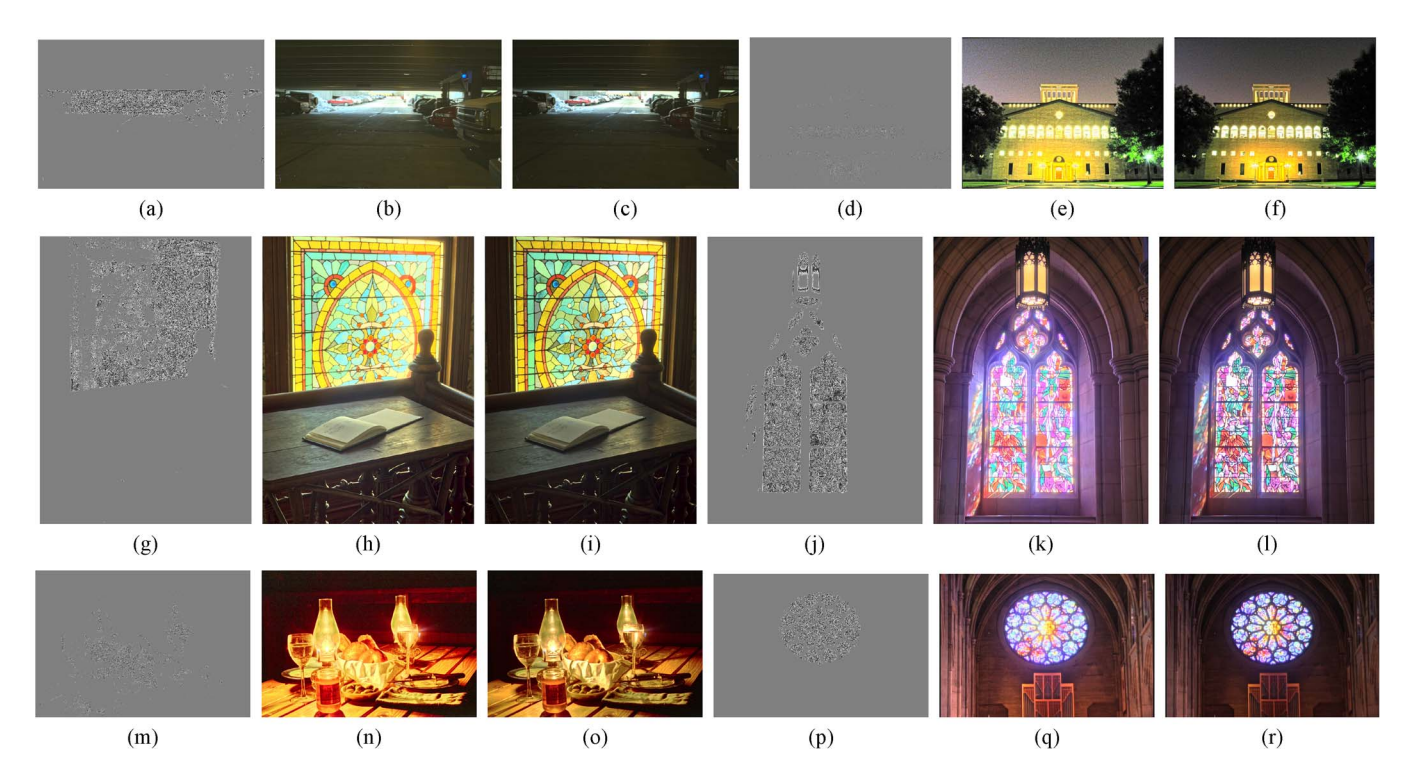


Fig. 3. Comparison of local tone-mapping algorithms with/without the proposed saliency-aware weighting (2). (b), (e), (h), (k), (n), and (q) Tone-mapped images by a local tone-mapping algorithm without the proposed saliency-aware weighting (2). (c), (f), (i), (l), (o), and (r) Tone-mapped images by the proposed local tone-mapping algorithm.

halo artifacts in the tone-mapped images by using the guided filter in [18]. The tone-mapped images by the proposed filter are comparable to those tone-mapped images by the global optimization method in [15], while the complexity of the proposed filter is much lower than that of the global optimization method in [15]. Even though the local tone-mapping algorithm in [13] and [25] can avoid halo artifacts from appearing in the tone-mapped images, it cannot preserve fine details as well as other three local tone-mapping algorithms.

The efficiency of the proposed saliency-aware weighting in (2) is then evaluated. It is worth noting that the saliencyaware weighting is involved in both the decomposition of  $L_h$ and the compression of  $L_b$ . The four different combinations are the following: 1) The saliency-aware weighting  $\Gamma_b(p)$  is neither used in the decomposition of  $L_h$  nor the compression of  $L_b$ ; 2) the saliency-aware weighting  $\Gamma_b(p)$  is only used in the decomposition of  $L_h$ ; 3) the saliency-aware weighting  $\Gamma_b(p)$ is only adopted in the compression of  $L_b$ ; and 4) the saliencyaware weighting  $\Gamma_b(p)$  is used in both the decomposition of  $L_h$  and the compression of  $L_b$ . They are compared by testing one HDR image. It is shown in Fig. 2(b) and (c) that more fine details are preserved in attention-salient regions by using the saliency-aware weighting  $\Gamma_b(p)$ . The attention-salient regions are also better exposed in the tone-mapped image. Therefore, the visual quality of the tone-mapped image, especially the attention-salient regions, is improved. Finally, the proposed local tone-mapping algorithm, i.e., the fourth method, is compared with the proposed local tone-mapping algorithm without consideration of saliency-aware weighting, i.e., the first method by testing six HDR images. It is illustrated in Fig. 3 that the same conclusion can be drawn. Therefore, the proposed

saliency-aware weighting can improve the visual quality of tone-mapped images.

### V. CONCLUSION AND DISCUSSION

Novel saliency-aware weighting and edge-aware weighting have been proposed for HDR images in this paper. They were applied to design a new local tone-mapping algorithm for the display of HDR images on display devices with limited dynamic ranges. Experimental results show that halo artifacts could be avoided from appearing in the tone-mapped image and the visual quality of the tone-mapped image, especially the attention-salient regions, is improved.

It should be pointed out that this paper has focused on incorporation of saliency-aware weighting and edge-aware weighting into local tone-mapping algorithms for HDR images. An interesting research topic is on the improvement of visual saliency models via the utilization of the HDR images. This topic will be investigated in our future research.

# REFERENCES

- P. E. Debevec and J. Malik, "Rendering high dynamic range radiance maps from photographs," in *Proc. SIGGRAPH*, Los Angeles, CA, USA, Aug. 1997, pp. 369–378.
- [2] J. Tsotsos, "Analyzing vision at the complexity level," *Behav. Brain. Sci.*, vol. 13, no. 3, pp. 423–445, Mar. 1990.
- [3] A. Borji, D. N. Sihite, and L. Itti, "Quantitative analysis of human-model agreement in visual saliency modeling: A comparative study," *IEEE Trans. Image Process.*, vol. 22, no. 1, pp. 55–69, Jan. 2013.
- [4] S. Grgic, M. Grgic, and B. Zovko-Cihlar, "Performance analysis of image compression using wavelets," *IEEE Trans. Ind. Electron.*, vol. 48, no. 3, pp. 682–695, Jun. 2001.

- [5] P. Y. Hsiao, C. L. Lu, and L. C. Fu, "Multilayered image processing for multiscale Harris corner detection in digital realization," *IEEE Trans. Ind. Electron.*, vol. 57, no. 5, pp. 1799–1805, May 2010.
- [6] J. Li, Y. H. Tian, T. J. Huang, and W. Gao, "Probabilistic multi-task learning for visual saliency estimation in video," *Int. J. Comput. Vis.*, vol. 90, no. 2, pp. 150–165, Nov. 2010.
- [7] S. Y. Chen, G. J. Luo, X. Li, S. M. Ji, and B. W. Zhang, "The specular exponent as a criterion for appearance quality assessment of pearllike objects by artificial vision," *IEEE Trans. Ind. Electron.*, vol. 59, no. 8, pp. 3264–3272, Aug. 2012.
- [8] C. Y. Chang and H. Lie, "Real-time visual tracking and measurement to control fast dynamics of overhead cranes," *IEEE Trans. Ind. Electron.*, vol. 59, no. 3, pp. 1640–1649, Mar. 2012.
- [9] H. L. Zhuang, K. S. Low, and W. Y. Yau, "Multichannel pulse-coupled-neural-network-based color image segmentation for object detection," *IEEE Trans. Ind. Electron.*, vol. 59, no. 8, pp. 3299–3308, Aug. 2012.
- [10] J. Garcia et al., "Directional people counter based on head tracking," IEEE Trans. Ind. Electron., vol. 60, no. 9, pp. 3991–4000, Sep. 2013.
- [11] E. Reinhard, G. Ward, S. Pattanaik, and P. E. Debevec, High Dynamic Range Imaging: Acquisition, Display and Image-Based Lighting. San Mateo, CA, USA: Morgan Kaufmann, 2005.
- [12] R. Fattal, D. Lischinski, and M. Werman, "Gradient domain high dynamic range compression," ACM Trans. Graphics, vol. 27, no. 3, pp. 67:1–67:10, Jul 2002
- [13] E. Reinhard, M. Stark, P. Shirley, and J. Ferwerda, "Photographic tone reproduction for digital images," ACM Trans. Graphics, vol. 21, no. 3, pp. 267–276, Jul. 2002.
- [14] A. Adams, *The Print*. ser. The Ansel Adams Photography series. New York, NY, USA: Little, Brown and Company, 1983.
- [15] Z. Farbman, R. Fattal, D. Lischinski, and R. Szeliski, "Edge-preserving decompositions for multi-scale tone and detail manipulation," ACM Trans. Graphics, vol. 21, no. 3, pp. 249–256, Aug. 2008.
- [16] F. Durand and J. Dorsey, "Fast bilateral filtering for the display of high-dynamic-range images," ACM Trans. Graphics, vol. 21, no. 3, pp. 257–266, Jul. 2002.
- [17] C. Tomasi and R. Manduchi, "Bilateral filtering for gray and color image," in *Proc. Int. Conf. Comput. Vis.*, Bombay, India, Jun. 1998, pp. 836–846.
- [18] K. He, J. Sun, and X. Tang, "Guided image filtering," *IEEE Trans. Pattern Anal. Mach. Learn.*, vol. 35, no. 6, pp. 1397–1409, Jun. 2013.
- [19] L. Itti, C. Koch, and E. Niebur, "A model of saliency-based visual attention for rapid scene analysis," *IEEE Trans. Pattern Anal. Mach. Intell.*, vol. 20, no. 11, pp. 1254–1259, Nov. 1998.
- [20] T. Judd, K. Ehinger, F. Durand, and A. Torralba, "Learning to predict where humans look," in *Proc. 12th IEEE Int. Conf. Comput. Vis.*, Kyoto, Japan, Dec. 2009, pp. 2106–2113.
- [21] F. Perazzi, P. Krahenbuhl, Y. Pritch, and A. Hornung, "Saliency filters: Contrast based filtering for salient region detection," in *Proc. IEEE Int. Conf. Comput. Vis.*, Providence, RI, USA, Jun. 2012, pp. 733–740.
- [22] S. Lu and J. H. Lim, "Saliency modeling from image histograms," in *Proc.* 12th Eur. Conf. Comput. Vis., Florence, Italy, Oct. 2012, pp. 321–332.
- [23] S. Lu, C. Tan, and J. H. Lim, "Robust and efficient saliency modeling from image co-occurrence histograms," *IEEE Trans. Pattern Anal. Mach. Learn.*, vol. 36, no. 1, pp. 195–201, Jan. 2014.

- [24] R. Shen, I. Cheng, and A. Basu, "QoE-based multi-exposure fusion in hierarchical multivariate Gaussian CRF," *IEEE Trans. Image Process.*, vol. 22, no. 6, pp. 2469–2478, Jun. 2013.
- [25] E. Reinhard, "Parameter estimation for photographic tone reproduction," J. Graphics Tools, vol. 7, no. 1, pp. 45–51, Nov. 2003.
- [26] J. Kuang, H. Yamaguchi, C. Liu, G. M. Johnson, and M. D. Fairchild, "Evaluating HDR rendering algorithms," ACM Trans. Appl. Perception, vol. 2, no. 4, pp. 9:1–9:27, Jul. 2007.
- [27] Z. Wang, A. C. Bovik, H. R. Sheikh, and E. P. Simoncelli, "Image quality assessment: From error visibility to structural similarity," *IEEE Trans. Image Process.*, vol. 13, no. 4, pp. 600–612, Apr. 2004.
- [28] L. M. Hurvich and D. Jameson, *The Perception of Brightness and Darkness*. Boston, MA, USA: Allyn & Bacon, 1966.
- [29] T. O. Aydin, R. Mantiuk, K. Myszkowski, and H. P. Seidel, "Dynamic range independent image quality assessment," ACM Trans. Graphics, vol. 27, no. 3, p. 69, Aug. 2008.



**Zhengguo Li** (SM'03) received the B.Sci. and M.Eng. degrees from Northeastern University, Shenyang, China, in 1992 and 1995, respectively, and the Ph.D. degree from Nanyang Technological University, Singapore, in 2001.

He is currently with the Agency for Science, Technology, and Research, Singapore. He is the coauthor of one monograph and approximately 60 journal papers. He is the holder of six patents. His research interests include mobile imaging, video processing and delivery, and hybrid systems.

Dr. Li served as the General Chair of IEEE ICIEA 2011, Technical Brief Co-Chair of SIGGRAPH Asia 2012, and Workshop Chair of IEEE ICME 2013. He was an Invited Lecturer by the 2011 IEEE Signal Processing Summer School and a Distinguished Invited Lecturer by IEEE INDIN 2012.



**Jinghong Zheng** received the B.Sci. degree in electronic engineering from the Beijing Institute of Technology, Beijing, China, in 2000, and the Ph.D. degree in electronic and electrical engineering from Nanyang Technological University, Singapore, in 2006.

She has been a Scientist with the Signal Processing Department, Institute for Infocomm Research, A\*STAR, Singapore, since 2006. Her research interests include high dynamic range imaging, image fusion, error concealment/resilience of H.264 video,

region of interesting video coding, scalable video coding, and video streaming.